Strength and durability of carbon fibre loops

Ing. Viktor Kulíšek

Abstrakt

Příspěvek se zabývá pevností a životností mechanických spojů kompozitních součástí. Je zde popsána problematika vrubu v anizotropním materiálu a jeho vliv na výslednou pevnost, který je mnohem větší než u klasických izotropních materiálů, zvlášť dojde-li při jeho výrobě k přerušení vláken. Integrované spoje kompozitních součástí tuto nevýhodu částečně odstraňují. Za modelový typ integrovaného spoje kompozitních součástí vyrobených technologií navíjení vláken byla zvolena vláknová smyčka z uhlíkových vláken. Jsou prezentovány výsledky experimentálních statických a únavových zkoušek tahově namáhaných smyček, včetně výpočtových analýz metodou konečných prvků. Jejich cílem je ukázat vliv geometrických parametrů na výslednou pevnost a životnost a představit možné pevnostní hypotézy použitelné pro predikci pevnosti spoje.

Klíčová slova

Kompozity, spoje, vláknové smyčky

1. Introduction

Composites from long fibres and epoxy resin are becoming important engineering material, excelling in a stiffness/weight ratio. One of the most critical areas of the composite parts design is the problematic of joining. For composite specimens, mostly two types of joints are used: bonded joints or mechanical joints (bolting, riveting). In this article, focus on mechanical joints will be held.

Generally, introduction of holes into a part brings stress concentration factors, which causes strength decrease. In a composite material, the strength decrease is more rapid than for classic isotropic materials. This is caused mostly by two reasons:

- Fibre breakage and discontinuity – due to the hole drilling.
- Brittle behaviour of fibres, which prevents plastic deformation in the concentrator area.

In [1] is said that a tensile loaded composite part with a hole has from 40 % to 60 % lower strength comparing the same part without hole. If this part is loaded in compression, the strength is lowered about 15 %.

One of the possibilities of the joint strength improvement is in the application of integrated joints. Integrated joints are prepared during the composite part manufacturing so that no fibres are cut. In Fig. 1 is shown a difference between composite laminate with integrated and machined hole. Their usage can bring much more efficient load transfer, as is demonstrated in Fig. 2, where is shown a difference in obtained maximal tensile force between laminate cylinder with integrated and machined holes.

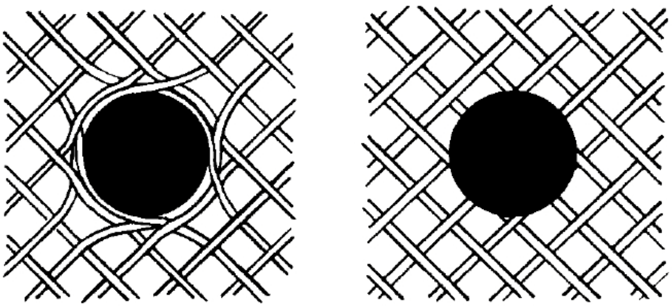

Fig. 1. *Braided vs cut hole in fibre composite*

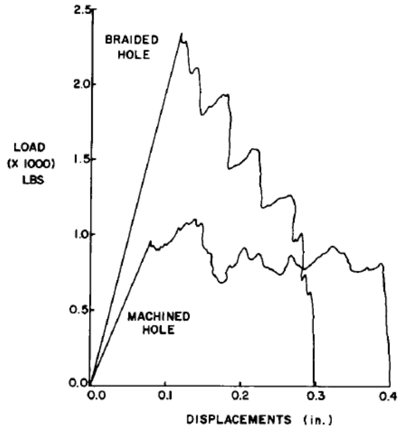

Fig. 2. *Strength increase due to the usage of braided holes – cylinders with pined holes in tension [2]*

A technology for manufacturing of integrated joins by filament winding technology was developed by CompoTech Plus company in a cooperation with CTU in Prague. By this method, a fibre tow is wrapped directly around the shape of a pin. It has been used for example for joints in hydraulic cylinders [3], composite spindles and other applications, as is shown in Fig. 3. Application of integrated joints can be found also in a civil engineering, where fibre loops are used as stiffeners for bending-loaded beams [4].

Fig. 3. *Integrated high-performance joints on products of CompoTech Plus company*

A fibre loop was selected as a model of a composite-metal wrapped pin joint. Static and fatigue experiments were done on tensile-loaded fibre loops from standard high-strength carbon fibres during a long-term research project at CTU

2. Experimental specimens

Experimental specimens were made from high strength carbon fibres Torayca T700 k12 and epoxy matrix. Specimens were manufactured in CompoTech Plus company. Loops were manually created by a filament winding technology. Specimens were placed at a room conditions for next 6 hours after loops manufacturing. Then, they were placed into an oven for a 24 hours long stabilization process at 40°C temperature. After that, 12 hours hardening process at 100°C temperature was used. Fibre volume fraction of specimens was between 49 and 70 %.
In Fig. 4 is shown a sketch of experimental specimens with dimensions description. Pictures of specimens are shown in Fig. 5.

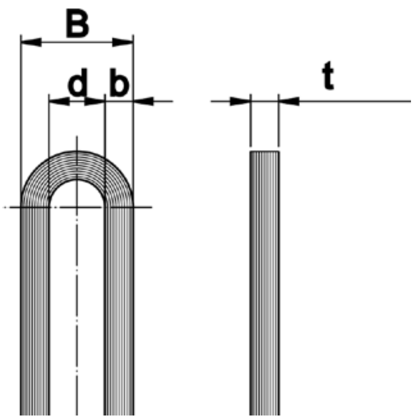

***Fig. 4**. Geometry of fibre loops*

Fig. 5. *Carbon fibre loops*

Due to the requirement of the behaviour description as a function of geometry, following specimens were tested:

- Inner diameter d 10, 20, 30 mm
- Number of fibre tows 6, 9, 12, 18, 30, 42 (corresponding to the loop thickness b=1.0 – 7.0 mm)
- Loop width approx. 5 mm

In table 1 are shown material properties of uni-directional composite layer made from T700/E with fibre volume fraction close to 60 %. These values were used for numerical analysis by finite element method.

***Table 1.** – Material properties of the composite T700/E with fibre volume fraction V_f=59%*

E_1	E_2=E_3	G_{12}=G_{13}	G_{23}	ν_{12}=ν_{13}	ν_{23}
131 GPa	8,2 GPa	4,4 GPa	3,6 GPa	0,25	0,38

3. Static experiments

Static experiments were made in laboratories of the Department of mechanics, biomechanics and mechatronics at CTU in Prague. For experiments, Heckert FPZ 100/1 machine was used. Static tests were run in a displacement control mode with a load cell speed 0.5 mm/sec in normal laboratory conditions. During experiments, force and displacement values were captured by LVDT. Picture of static experiments of carbon fibre loop is shown in Fig. 6.

***Fig. 6.** Tensile test of fibre loop specimen*

Result of static experiments of loops with inner diameter 10 mm were published in [15], [16], [17]. These values are here extended with results of loops with inner diameter 20 and 30 mm. Values of maximal tensile force for fibre loops of inner diameter 10, 20 and 30 mm are shown in Fig. 7.

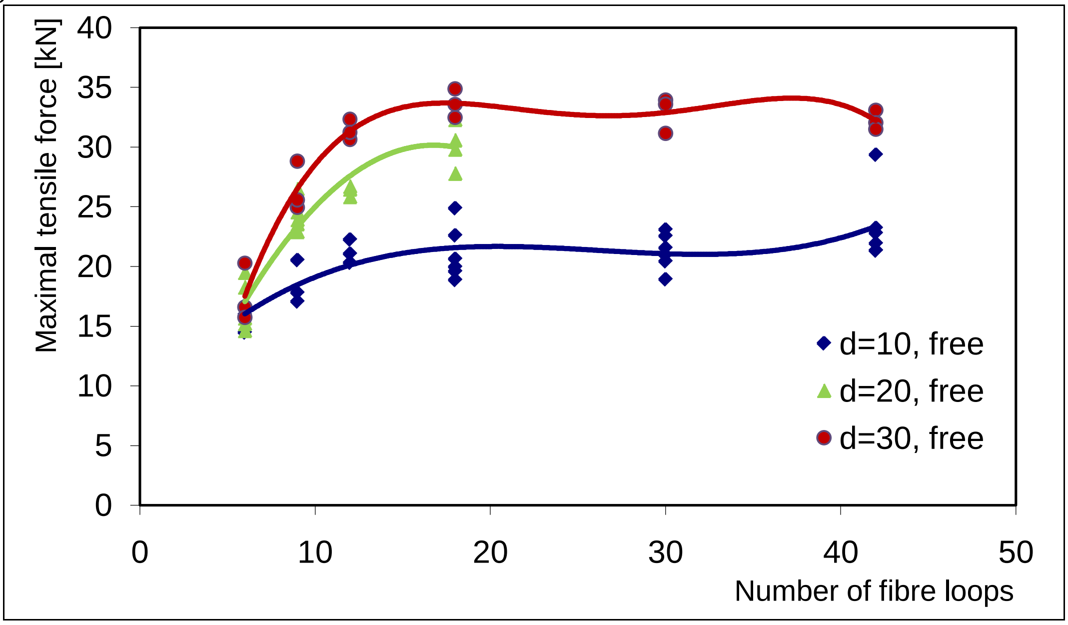

Fig. 7. *Maximal tensile force for fibre loops with free sides*

For engineering purposes, maximal tensile force was recalculated to a nominal tensile stress σ_{nom} in the straight part of specimen or to a nominal tensile stress σ_{fnom} in fibre tows in the straight part of specimen. Due to the variation of specimen cross-section and also the variation of the fibre volume fraction, the second type of data post-processing was used. A ratio of nominal tensile stress in the fibre tows and the fibre tows tensile strength is presented in Fig. **8**.

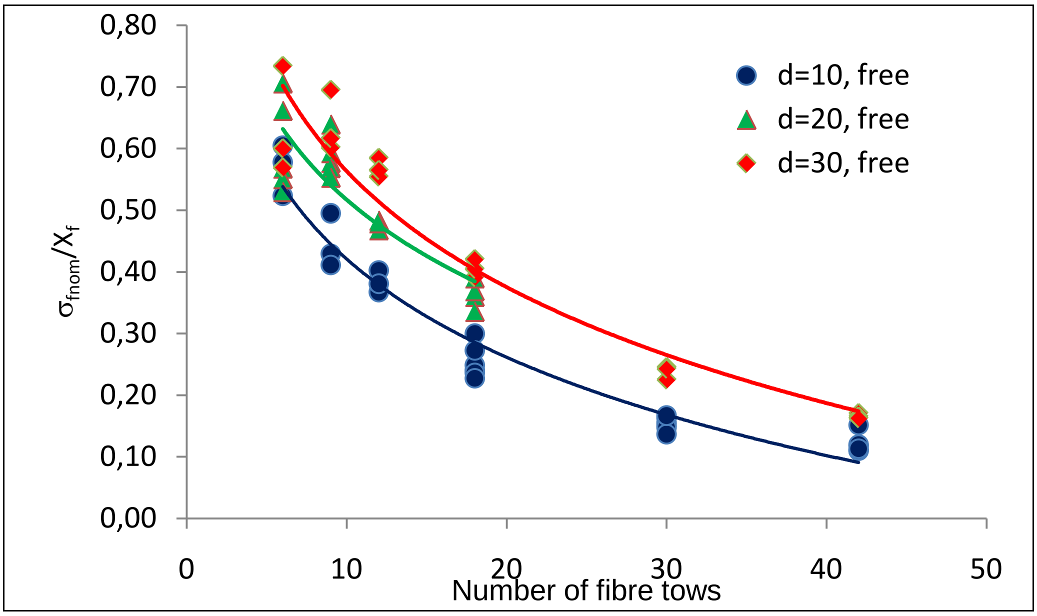

Fig. 8. *Ratio on the nominal tensile stress in fibres vs fibre tensile strength*

Following conclusions can be made from the presented results:

- Material usage is decreasing with the increasing number of fibre tows. Maximal reasonable number of tows was 18, usage of the thicker loops would not lead to the higher maximal force as can be seen from the Fig. 7.
- Application of the loops with bigger inner diameter leads to the higher transferred loads and more efficient material usage. The difference in the material usage between specimens with d=10 mm and d=20 mm was approximately between 10 and 15%. The next extension of the inner diameter lead to a smaller increase of the material usage as the difference between d=20 mm and d=30 mm was approximately between 5 and 7%.

Following design recommendation can be made: use pins with maximal dimensions that are possible. Higher transferred load may be reached by the usage of higher number of joints, not by the extension of the joint thickness. If the construction doesn't allow the application of more joints, application of parallel composite lugs can lead to higher transferred loads, as is presented in [5].

4. Fatigue behaviour

Fatigue experiments were made in the laboratories of Department of mechanics, biomechanics and mechatronics. An electro-magnetic resonance machine Amsler 10 HFP 422 was used as this experimental frame was able to load specimens at high frequencies. For the fibre loops specimens, a loading frequency was about 55 Hz. A high frequency may influence results of experiments, as it leads to the increase of the specimen temperature, which causes the decrease of the specimen lifetime. Experiments at the standard load frequency (5 Hz) will be done in the future.

Experiments for the detection of fatigue behaviour were so far done only on the fibre loop specimens of inner diameter d=10 mm. Specimens were loaded in force-controlled cycles with $R=\sigma_{min}/\sigma_{max}=0.05$. In Fig. 9 is shown a clamped specimen during cycling.

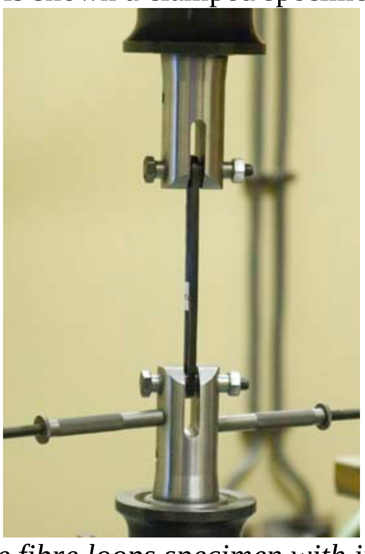

Fig. 9. *Fatigue test of the fibre loops specimen with inner diameter d=10 mm*

Experimental results are shown in Fig. 10 and Fig. 11. In Fig. 10 is shown a F_{max}-N diagram, where F_{max} is a maximal value of force during cycle. For a data post-processing purposes, F_{max} was recalculated to the nominal tensile stress σ_{fnom} in the fibre tows in the straight part of specimen. For the better interpretation of results, a ratio of the stress σ_{fnom} over the fibre tows tensile strength Xf is presented in Fig. 11.

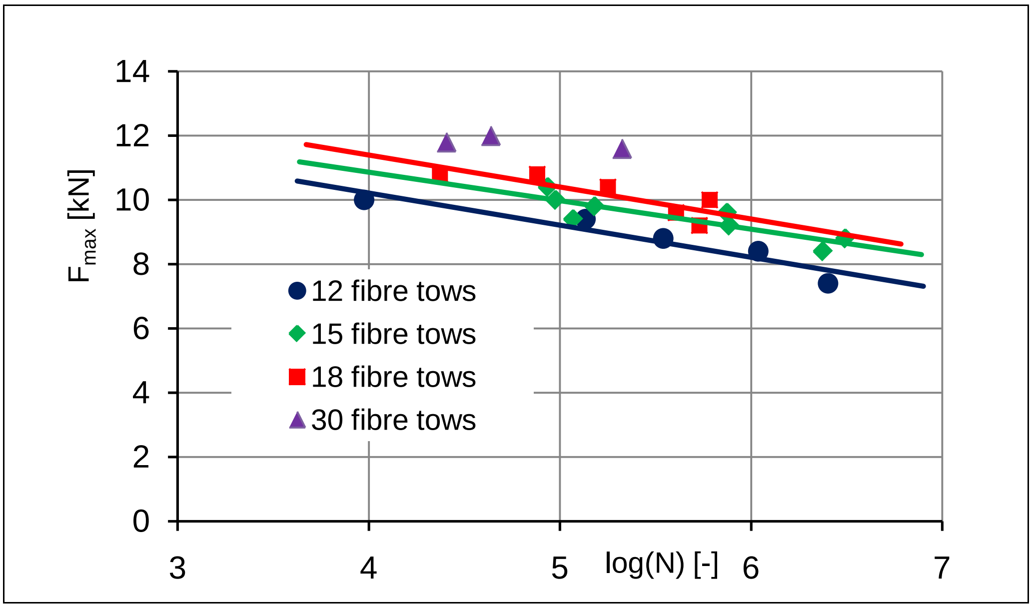

Fig. 10. *Experimental results of carbon fibre loops with inner diameter d=10 mm*

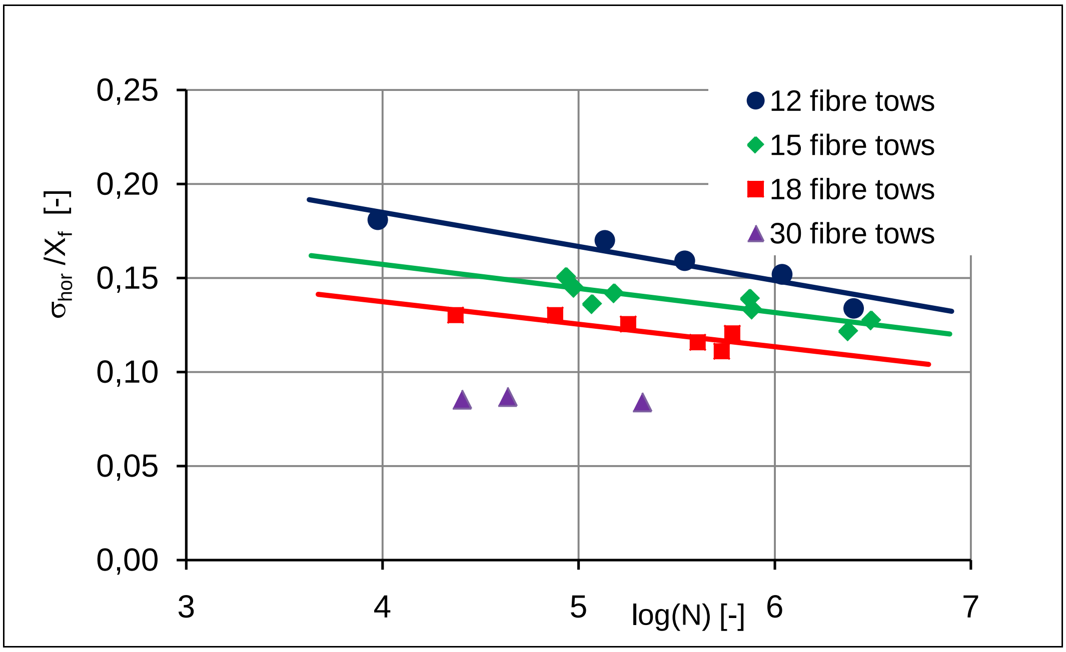

Fig. 11. *S-N curve of carbon fibre loops with inner diameter d=10 mm*

As is clearly shown from Fig. 10 and Fig. 11, specimens with a high thickness are not effective for the load transfer. The difference in maximal force between specimens from 12 loops and 18 loops is about 1.2 kN for the same durability. Especially, the application of thick loops that were made from 30 fibre tows was ineffective.
Fatigue strength for the lifetime about 10^6 cycles is approximately 40% of static strength.

5. Numerical analysis of carbon-fibre lugs

Finite element method was used for the analysis of experimental specimens. Finite element model of a fibre loop specimen was described in [18] as the model was used to analyse a stress distribution field in fibre loop specimens of inner diameter d=10 mm. This model was recently upgraded for specimens with inner diameter d=20 mm and d=30 mm.

For numerical analysis, Abaqus Standard software in version 6.8.2 was used. FE model of fibre loop is shown in Fig. 12. Model was build from two parts. The first part represented the fibre loop, the second part represented a steel pin. Due to the application of a model symmetry, only the one eighth from the fibre loop specimen was modelled. The loop specimen was meshed with quadratic solid elements. The pin was modelled as an analytical rigid body and was loaded by a force. Contact interaction between the pin and fibre loop was defined. In normal interaction mode, a "hard" definition was used. In tangential interaction mode, friction was used.

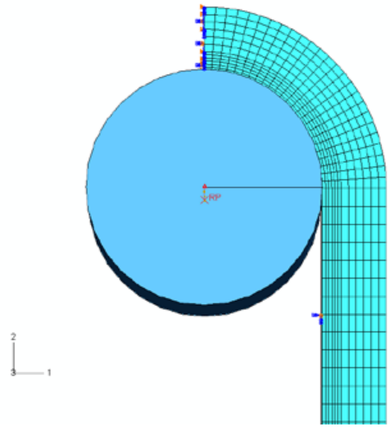

Fig. 12. *Finite element model of loaded fibre loop specimen, d=10mm*

Finite element analysis was used for the determination of stress distribution in horizontal and vertical section of specimen and in the area of maximal tensile load in curved section of loop as is shown in Fig. 13. Position of maximal tensile load, marked by the angle ϕ_m in a cylindrical coordination system, is depending on the loop geometry. It is decreasing with the increase of inner diameter d or the decrease of number of fibre loops.

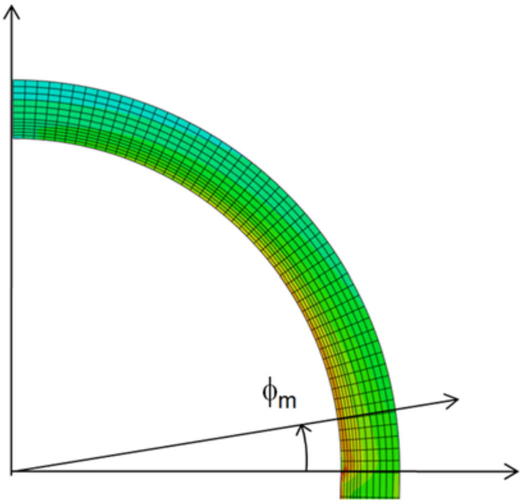

Fig. 13. *Paths for the stress evaluation*

In Fig. 14 are shown tensile stress distributions for specimens from 18 fibre loops loaded by pin of size d=10 mm, d=20 mm and d=30 mm. It can be clearly seen how the stress peak is moving in the direction to the horizontal section.

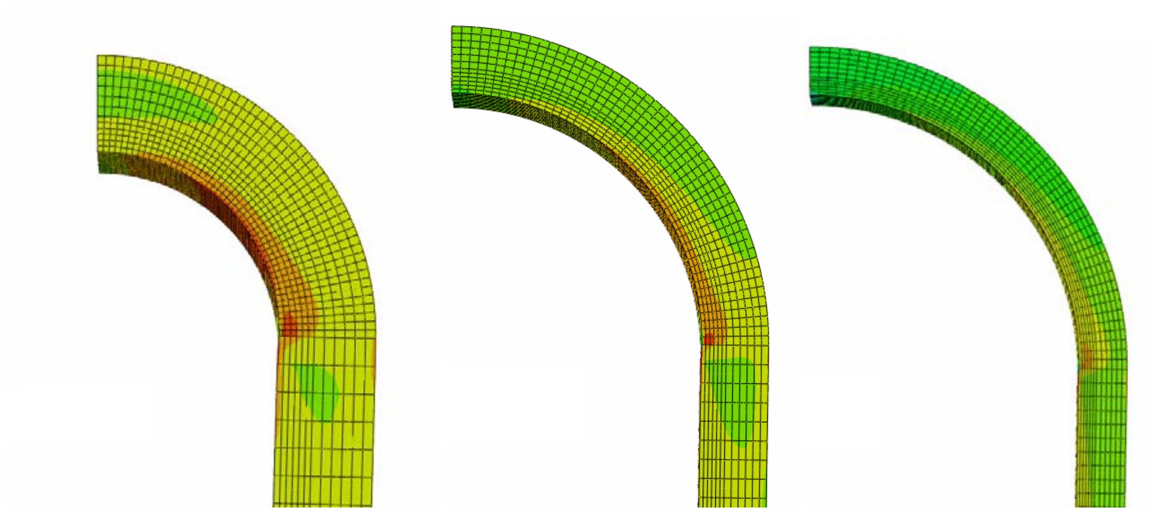

Fig. 14. *Stress in longitudinal direction for loop with d=10 mm, 20 mm 30 mm (from left side)*

In Fig. 15 is shown a comparison of the stress concentration factor of experimental specimens with inner diameter d=10, 20 and 30 mm. The concentration factor was defined by a ratio of maximal tensile stress on the inner radius of the specimen over a nominal tensile stress in the straight part of the specimen. The value of the stress concentration factor for specimens loaded by pin with diameter d=10 mm is high even for small number of fibre tows. Also its gradient is much higher than for the specimens loaded by pin with d=20 or 30 mm. The difference between specimens loaded by pin with d=20 and 30 mm is small comparing the shift between specimens with pin of diameter d=10 and 20 mm. This can be taken as a verification of conclusions from the results of static experiments.

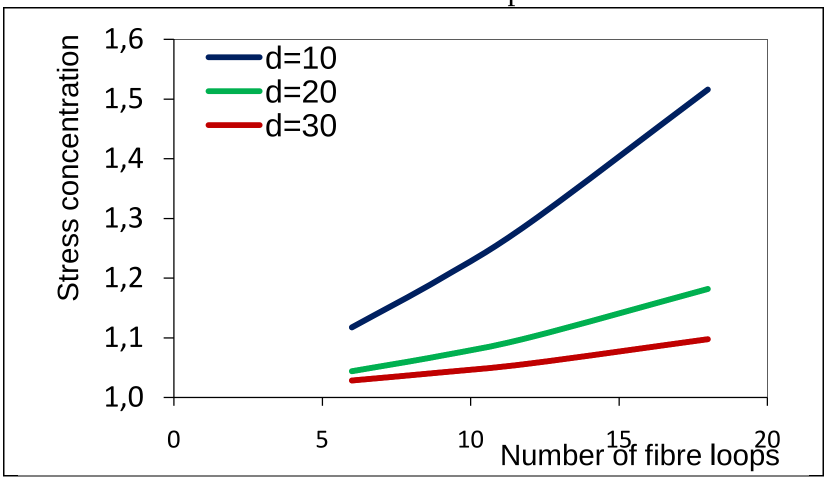

Fig. 15. *Stress concentration factor*

6. Basic criteria for strength prediction

The most usual failures of pin-loaded composites are a net-tension failure, a shear-out failure and a bearing failure. Classic criteria for laminate failures, like a maximal stress criterion or a criterion of maximal deformation, cannot be used for a strength prediction of notched fibre composites. Their usage would lead to under or over-estimation of strength prediction, depending on the distance of evaluated point from notch.

Whitney and Nuismer [6] developed two basic criteria Point stress criterion (PSC) and Average stress criterion (ASC) for the strength prediction of tensile-loaded laminates with holes. These criteria were based on a characteristic length method, comparing a local stress in the characteristic distance d with the tensile strength of un-notched laminate, where the characteristic length was taken as a material property. These criteria were extended, in [7], [8], characteristic length was defined not only as a function of material, but also as a function of specimen geometry. PSC or ASC are capable to give a good option for the determination of the strength of tensile-loaded specimen with a circular hole that is not loaded in contact.

For a pin-loaded composite specimen, Chang [9], [10] developed a characteristic curve method, determined from characteristic lengths. Failure criterion has to be applied for every point of this curve, given by (1). In Fig. 16 is shown a demonstration of the characteristic curve for a pin-loaded laminate. Another possibility for the determination of the maximal transferred load is the application of accumulative damage methods [11], [12], or in the use of "Failure area index" [13]. Recently, a work [14] on a wrapped composite/steel pin joint was published where LARC criterion with some numerical modifications was used.

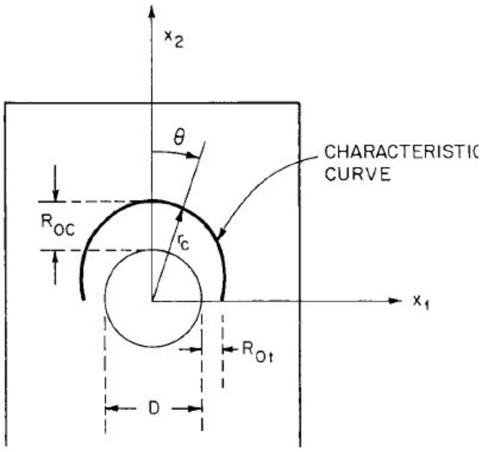

Fig. 16. *Schematic description of the characteristic curve*

$$r_c(\phi) = \frac{D}{2} + R_{ot} + (R_{oc} - R_{ot})\cos\phi \ , \tag{1}$$

where R_{ot} resp. R_{oc} is characteristic length in tension, resp. compression. These values should be determined from experimental tests, however it should be taken into account, that they are not material constants, but their value is depends on material and specimen dimensions.

For the application in the prediction of the fibre loop strength was used Chang criterion of the characteristic curve [9]. Only compressive matrix cracking mode and fibre breakage mode were taken into account. According to [10], combination of both modes can be simplified for linear elastic composite into eq. (2).

$$\left(\frac{\sigma_x}{X_t}\right)^2 + \left(\frac{\sigma_{xy}}{S_c}\right)^2 = e_f^2 \ , \tag{2}$$

where σ_x, resp. X_t are the longitudinal tensile stress, resp. strength in each ply, σ_{xy}, resp. S_c are the shear stress, resp. strength in each ply of laminate. The criterion states that the layer fails by either fibre breakage or fibre-matrix shearing, when $e_f \geq 1$.

Stress distribution in the fibre loops were determined by FE simulations, as is described in previous chapter. For the strength prediction, specimens were loaded by a force that was corresponding to the maximal tensile force from static experiments. Then was criterion e_f from (2) evaluated along the stress patch in the radial direction that was starting from the point of maximal tensile load in the curved part of specimen, as is shown in Fig. 13. This approach using the section of maximal loading should be correspond to the characteristic curve approach. It was not possible to determine whole characteristic curve, due to the lack of precise analytical model and especially due to the inaccuracy in the determination of characteristic length parameters. These values can be determined from lamina type specimens, it is almost impossible to measure these values from the fibre tows type of specimens, mainly due to the problems with the clamping of specimen.

In Fig. 17 is shown a comparison of e_f criterion for specimens that were loaded by a pin of diameter d=10 mm, in Fig. 18 is shown analogical comparison of e_f criterion for specimens loaded by the pin of diameter d=20 mm. Parameter of longitudinal tensile strength X_f=2520 MPa and shear strength S_c=80 MPa was used for the criterion evaluation. However, application of these values is problematic as they were not determined experimentally, but from the fibre manufacturer sources and literature.

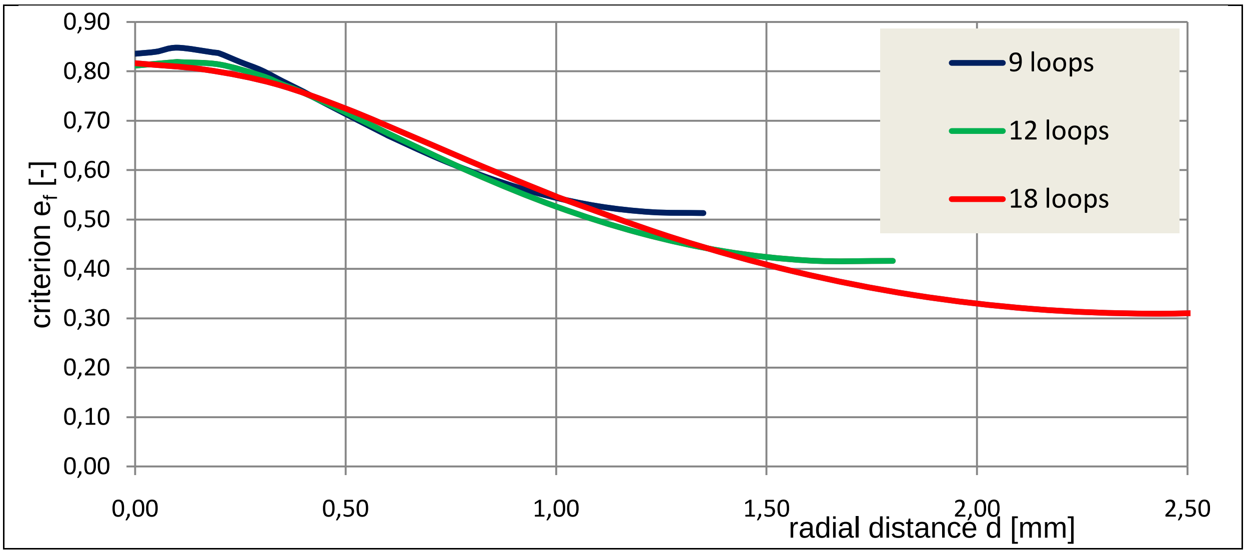

Fig. 17. *Failure criterion for specimens loaded by pin with d=10 mm*

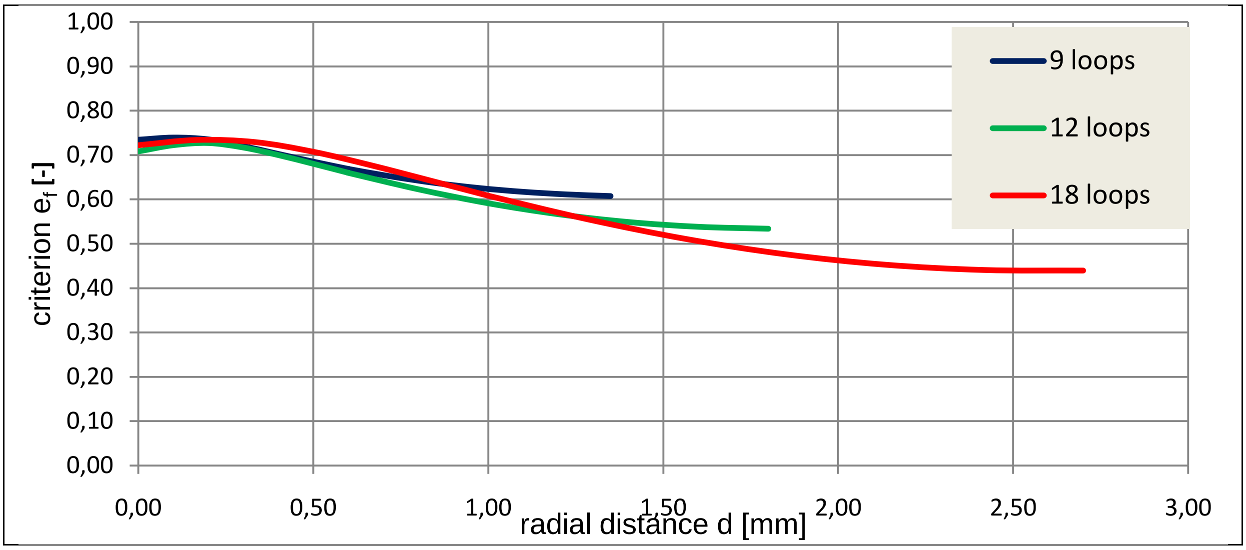

Fig. 18. *Failure criterion for specimens loaded by pin with d=20 mm*

It can be clearly seen that the criterion e_f has not reached value of 1. From the criteria definition, the value should be equal or greater than 1 for the layer failure. That demonstrates that application of this criterion was not very successful. However, making a relative comparison, a good agreement in the criterion value was obtained in the characteristic distance d_c=0.42 mm for the specimens loaded by pin of size 10 mm, and in the characteristic distance d_c=0.25 mm for the specimens loaded by pin of size 20 mm. That is confirming the fact that the characteristic distance is a function of ratio d/b as it was a function of ratio D/W in laminates of width W and hole of diameter D.

The agreement in criterion e_f means that the stress field or its influence of the specimen failure is similar for the loops of different thickness in the distance d_c. Also the value of criterion e_f ~0.75 is similar for the specimens loaded by pin of size d=10 mm and d=20 mm.

From this criterion, approximate strength may be predicted by following algorithm:

1) FE model of the loop of required geometry will be made.
2) Radial path for stress analysis will be made from the point of maximal tensile load on the inner radius.
3) Specimen will be loaded by a nominal force so that the stress along the path can be analysed.
4) In the characteristic distance d_c will be determined the tensile and shear stress and a nominal criterion e_{fnom}. Using assumptions of linear analysis, a maximal force will be determined from criterion e_f.

However, further research has to be made to confirm these conclusions. Improvement in strength parameters X_f and S_c has to be made, also it's necessary to test more specimens to improve the statistical set for data post-processing.

7. Conclusion

Static and fatigue results of carbon fibre loop specimen were presented. Effective load transfer can be achieved only by the application of thin loops. Experimental data showed that the increase of the transferred load was marginal while using the specimens with more than 18 fibre loops. Static strength of specimens made from 18 loops was approximately 32-34 % of nominal fibre tensile strength for specimens loaded by pin of size d=10 mm and approx. 46-48 % for specimens loaded by pin of size d=30 mm. Further increase of the loop inner diameter would not bring distinct increase of the material usage.

Results of fatigue experiments confirmed the conclusions from static tests. Fatigue strength of specimens made from 18 loops with inner diameter d=10 mm was about 12% of the nominal tensile fibre strength for the lifetime 10^6 cycles. Comparing the fatigue strength to the static strength, fatigue strength for the lifetime 10^6 cycles was about 40% of static strength.

Basic criterion derived from the characteristic curve and Yamada-Sun criterion was used for the determination of the characteristic distance d_c. A good agreement and possibility for the maximal load prediction was reached, however the application of this criterion has to be subject to the further research.

List of symbols

e_f	Failure criterion	[-]
D	Diameter of hole	[mm]
E_i	Young's modulus in the i-direction	[MPa]
F_{max}	Maximal force of fatigue loading	[kN]
R_{oc}	Characteristic length in compression	[mm]
R_{ot}	Characteristic length in tension	[mm]
S_c	Shear strength of composite	[MPa]
X_f	Tensile strength of the fibre tows	[MPa]
ϕ_m	Ange corresponding to the maximal tensile load in the curved part of specimen	[°]
σ_x	Longitudinal tensile stress	[MPa]
σ_{xy}	Shear stress	[MPa]

References

[1] Gay, D., Hoa, S.V., Tsai, S.W., *Composite Materials, Design and Applications*, CRC PRESS, 2003.

[2] Brookstein, D. S., Tsiang, T.-H.: Load-Deformation Behaviour of Composite Cylinders with Integrally-Formed Braided and with Machined Circular Holes. *Journal of Composite Materials*, 19, 1985, p. 476-487.

[3] Patent CS8907597, 1992.

[4] Patent US6209279, 2001.

[5] Schürmann, H.: *Konstruieren mit Faser-Kunststoff-Verbunden*. Springer-Verlag, 2005. 569 p., ISBN 3-540-40283-7.

[6] Whitney, J.M., Nuismer, R.J., Stress Fracture Criteria for Laminated Composites Containing Stress Concentrations, *Journal of Composite Materials*, 8, 1975, 253-265.

[7] Pipes, R.B., Wetherhold, R.C., Gillespie, J.W. Jr., Notched Strength of Composite Materials, *Journal of Composite Materials*, 1979, 13, p. 148-160.

[8] Kim, J.-K., Kim, D.-S.., Takeda, N., Notched Strength and Fracture Criterion in Fabric Composite Plates Containing a Circular Hole, *Journal of Composite Materials*, 29, 1995, 982-998.

[9] Chang, F.-K., Scott, A. S., Springer, G. S: Strength of Mechanically Fastened Composite Joints. *Journal of Composite Materials*, 16, 1982, p. 470-494.

[10] Chang, F.-K., Chang, K.-Y.: Post-Failure Analysis of Bolted Composite Joints in Tension and Shear-Out Mode Failure. *Journal of Composite Materials*, V. 21, 1987, p. 809-833.

[11] Sun, H.-T., Chang, F.-K., Qing, X., The Response o Composite Joints with Bolt-Clamping Loads. Journal of Composite Materials, 2002, 36, p. 47-92.

[12] Wang, H.-S., Hung, C.-L., Chang, F.-K.: Bearing Failure of Bolted Composite Joints.. *Journal of Composite Materials*, 30, 1996, p. 1284-1400.

[13] Choi, J.-H., Chun, Y.-J.: Failure Load Prediction of Mechanically Fastened Composite Joins. *Journal of Composite Materials,* V. 37, 2003, p. 2163-2177.

[14] Kottner, R., Kroupa, T., Laš, V., Blahouš, K.: Computational Model for Strength Analysis of Wrapped Pin Joint of Composite/Metal. *Bulletin of Applied Mechanics*, 4, 2008, p. 1-6.

[15] Růžička, M., Kulíšek, V. Turčič, B., Blahouš, K.: Statické a únavové zkoušky smyček z uhlíkových vláken. In *Únava a lomová mechanika 2008*, Žinkovy 14.04.2008, ISBN 978-80-7043-675-0.

[16] Růžička, M., Uher, O., Blahouš, K., Kulíšek, V., Dvořák, M.: Integrated High Performance Joint In Composite Vessels, In *Proceedings of the 16th International Conference on Composite Materials*, Kyoto 8.-13.8.2007.

[17] Růžička, M., Blahouš, K., Kulíšek, V., Turčič, B.: Pevnost smyčky ze svazku C-vláken. In *Vyztužené plasty*, roč. XXIV, Karlovy Vary 22-24.5.2007. Dům techniky Plzeň, s.r.o., s 69-75, ISBN 978-80-239-8857-4.

[18] Kulíšek, V., Růžička, M., Pinkas, J.: Pevnostní kritéria vláknové smyčky z uhlíkových vláken, In Proceedings *of the 8th Workshop of Applied Mechanics*, Praha 19.10.2007.